

BIFURCATION SET FOR A DISREGARDED BOGDANOV-TAKENS UNFOLDING. APPLICATION TO 3D CUBIC MEMRISTOR OSCILLATORS.

ANDRÉS AMADOR¹ AND EMILIO FREIRE² AND ENRIQUE PONCE³

ABSTRACT. We derive the bifurcation set for a not previously considered three-parametric Bogdanov-Takens unfolding, showing that it is possible express its vector field as two different perturbed cubic Hamiltonians. By using several first-order Melnikov functions, we obtain for the first time analytical approximations for the bifurcation curves corresponding to homoclinic and heteroclinic connections, which along with the curves associated to local bifurcations organize the parametric regions with different structures of periodic orbits.

As an application of these results, we study a family of 3D memristor oscillators, for which the characteristic function of the memristor is a cubic polynomial. We show that these systems have an infinity number of invariant manifolds, and by adding one parameter that stratifies the 3D dynamics of the family, it is shown that the dynamics in each stratum is topologically equivalent to a representant of the above unfolding. Also, based upon the bifurcation set obtained, we show the existence of closed surfaces in the 3D state space which are foliated by periodic orbits. Finally, we clarify some misconceptions that arise from the numerical simulations of these systems, emphasizing the important role played by the existence of invariant manifolds.

Bifurcation set, Bogdanov-Takens, homoclinic orbit, heteroclinic connection, Melnikov function, Memristor oscillators

1. INTRODUCTION

In planar systems, the existence of some local bifurcations may reveal the presence of other bifurcations of global character [13, 14] and the curves that determine these global phenomena are difficult to determine. This is, for instance, the case regarding the appearance of homoclinic or heteroclinic connections.

A homoclinic connection is an orbit of the system that joins a saddle equilibrium point to itself, and generally creates or destroys periodic orbits (see, for instance [35]). A heteroclinic connection joins two different equilibrium points of a system and the existence of this connection can determine changes in the basin of attraction of a positively invariant set.

Following [18], the techniques to study homoclinic orbits in planar vector fields were well developed during the 1920s in the works of Dulac. The fundamental idea is that the recurrent behavior near a connecting orbit should be studied in a fashion similar to that used in studying periodic orbits via a Poincaré return map. But there are some additional complications in the study of homoclinic orbits compared to that of periodic orbits which significantly complicate the analysis.

¹Facultad de Ingeniería y Ciencias, Departamento de Ciencias Naturales y Matemáticas, Pontificia Universidad Javeriana-Cali, Cali, Colombia.

^{2,3} Departamento de Matemática Aplicada, Escuela Técnica Superior de Ingeniería, Avda. de los Descubrimientos, 41092 Sevilla, Spain.

¹afamador@javerianacali.edu.co, ²efrem@us.es ³eponcem@us.es

Usually, the bifurcation curves of homoclinic and heteroclinic connections are studied by numerical continuation techniques [17, 18, 9, 36]. On the other hand, when a planar system can be written as a perturbed Hamiltonian system, we can calculate some Melnikov functions, introduced by Melnikov in [28], and under certain hypotheses, the zeros of the associated Melnikov function determine the existence of periodic orbits, homoclinic loops or heteroclinic connections, see for instance [8, 20, 3].

As show later, we will resort to such Melnikov functions for setting information on such global bifurcations curves in a two-parametric plane for a specific family of differential systems.

The normal form of the Bogdanov-Takens (see [35]) bifurcation is given by

$$\dot{x} = y, \quad \dot{y} = \mu_1 + \mu_2 x + x^2 \pm xy.$$

Following the classification proposed in [14], the deformation of codimension three of the previous normal form is given by the unfolding

$$(1) \quad \begin{aligned} \dot{x} &= y, \\ \dot{y} &= \mu_1 + \mu_2 x + \alpha x^3 + y(\mu_3 + \mu_4 x \pm x^2), \end{aligned}$$

The presence of this type of systems has been reported in different applications, see [16, 2, 24]. On the study of bifurcation phenomena in these systems many contributions have been made. In [15], the authors studied the global bifurcation diagram of the three-parameter family

$$\begin{aligned} \dot{x} &= y, \\ \dot{y} &= \mu_1 + \mu_2 x - x^3 + y(\mu_3 - 3x^2), \end{aligned}$$

and fixing $\mu_3 > 0$, they obtained analytical approximations to the bifurcation curves of the homoclinic orbits, by using Melnikov functions. Later on, the above work was quoted in [23], where a numerical analysis of the same model was performed. In [10, 12, 11], it is considered the system

$$(2) \quad \begin{aligned} \dot{x} &= y, \\ \dot{y} &= \mu_1 + \mu_2 x - x^3 + y(\mu_3 + \mu_4 x - x^2), \end{aligned}$$

and the authors showed that it can be written as a perturbed Hamiltonian system, reporting the maximum number of limit cycles. Later, by taking the parameter $\mu_4 = 0$ in (2), the authors in [4, 5, 7, 6] analyzed the system as a Liénard system, its local bifurcations were characterized, and a numerical study of the global bifurcations was done.

While all the above references dealt with the focus case, in this work we study the saddle case

$$(3) \quad \begin{aligned} \dot{x} &= y, \\ \dot{y} &= \mu_1 + \mu_2 x + x^3 + y(\mu_3 - 3x^2), \end{aligned}$$

which up to the best of our knowledge, seems to be a disregarded case with rather interesting dynamic behavior.

In fact, our motivation comes from the analysis of certain 3D memristor oscillators [1, 30, 22], where under specific hypotheses on the memristor characteristics, such system appears in a natural way after a dimensional reduction achieved thanks to the existence of a first integral.

The paper is organized in the following way. First, in section 2 we review the information that can be gained by means of a local analysis of the system. Our main results appear in section 3, where we apply Melnikov theory to approximate the homoclinic and heteroclinic curves on a convenient parameter plane. We obtain the global bifurcation set for system (3), by splitting such a plane in regions with different qualitative dynamical behavior. Next, in section 4, We show how the above analysis is useful for deriving all the possible responses of certain 3D canonical memristor oscillators, when the flux-charge characteristics function is a specific cubic polynomial, generalizing some results given in [1]. As one of the possible dynamical behaviors, we focus our attention in showing, thanks to the previous analysis, the existence of a topological sphere in the 3D phase-space completely foliated by periodic orbits. Thus, we confirm previous numerical results reported in [29, 25]. The necessity of incorporating rigorous techniques in the analysis of memristor oscillators is emphasized with the material of section 5, where following a similar procedure for the dimensional reduction of section 4, we can refute several recently published studies that report the existence of an infinite number of hidden attractors in a three-dimensional memristor-based autonomous Duffing oscillator. Some technical results are relegated to the appendix.

2. LOCAL BIFURCATIONS

In this section, we study the local bifurcations that occur in system (3). First, we note that the system is invariant under the transformation

$$(x, y, \mu_1, \mu_2, \mu_3) \rightarrow (-x, -y, -\mu_1, \mu_2, \mu_3).$$

Therefore, it is sufficient to study the bifurcation diagram for $\mu_1 > 0$. The equilibrium points of the system are of the form $(\bar{x}, \bar{y}) = (\tilde{x}, 0)$, being \tilde{x} a solution of the cubic $\mu_1 + \mu_2 x + x^3 = 0$, and its Jacobian matrix of is given by

$$(4) \quad J(x, y) = \begin{pmatrix} 0 & 1 \\ \mu_2 + 3x^2 - 6yx & \mu_3 - 3x^2 \end{pmatrix}.$$

Remark 1. *Note that for $\mu_3 \leq 0$ the divergence of system (3) does not change sign, thus from Bendixson's criterion [21], the system does not have periodic solutions.*

First, we provide a technical result that provides a study of the number of equilibria in system (3) and their topological nature.

Lemma 2. *Consider system (3), the following statements hold.*

- (a) *If $\mu_2 \geq 0$ or we have $\mu_2 < 0$ with $27\mu_1^2 + 4\mu_2^3 > 0$, then the system has only one equilibrium point.*
- (b) *If $\mu_2 < 0$ and $27\mu_1^2 + 4\mu_2^3 = 0$ we have two equilibrium points.*
- (c) *If $\mu_2 < 0$ and $27\mu_1^2 + 4\mu_2^3 < 0$, then the system has three equilibrium points $\mathbf{x}_i = (s_i, 0)$ with $i \in \{L, C, R\}$ such that*

$$(5) \quad s_L < -(-\mu_2/3)^{1/2} < s_C < (-\mu_2/3)^{1/2} < s_R,$$

and $s_L + s_C + s_R = 0$. Furthermore, \mathbf{x}_L and \mathbf{x}_R are saddles while \mathbf{x}_C is an antisaddle (node or focus).

Proof. We study the roots of the polynomial $p(x) = \mu_1 + \mu_2 x + x^3$. Since $p'(x) = \mu_2 + 3x^2$, if $\mu_2 \geq 0$ we obtain $p'(x) \geq 0$ and so the polynomial has only one root.

In the rest of the proof we assume $\mu_2 < 0$. The derivative $p'(x)$ vanishes at the points $x_{\pm} = \pm(-\mu_2/3)^{1/2}$ being a maximum and minimum local respectively, also a direct computation gives $p(x_{\pm}) = \mu_1 \mp 2(-\mu_2/3)^{3/2}$. When $p(x_-) < 0$ or $p(x_+) > 0$ the graph of $p(x)$ only crosses once the x -axis and so these inequalities provides the condition $27\mu_1^2 + 4\mu_2^3 > 0$, and the statement (a) follows. Assuming $p(x_-) = 0$ or $p(x_+) = 0$, the statement (b) follows.

Finally, if $p(x_+) < 0 < p(x_-)$ then we have three roots as indicated in (5). Moreover, using the relation between roots and coefficients of polynomials, we get

$$\mu_1 = -s_L s_C s_R, \quad \mu_2 = s_C s_L + s_C s_R + s_L s_R, \quad s_L + s_C + s_R = 0.$$

For the Jacobian matrix given in (4), we get $J(s_i, 0) = -(\mu_2 + 3s_i^2) = -p'(s_i)$. As we know that $p'(s_L) > 0$, $p'(s_C) < 0$ and $p'(s_R) > 0$, the conclusion follows and the proof is complete. \square

In the next result, we give a characterization of the local bifurcations of system (3) on the parametric plane (μ_2, μ_1) , assuming a fixed value of the parameter μ_3 . Note that we have put the μ_1 axis in the plane (μ_2, μ_1) vertically, being the μ_2 axis the horizontal one.

Proposition 3. *The following statements hold for system (3).*

(a) *Given $\mu_3 \in \mathbb{R}$ the parameter values in the set*

$$(6) \quad \varphi_{sn} = \{(\mu_2, \mu_1) : 27\mu_1^2 + 4\mu_2^3 = 0\},$$

correspond with saddle-node bifurcation points of equilibria. In particular, the system has a cusp bifurcation of equilibria at $\mu_2 = \mu_1 = 0$.

(b) *Given $\mu_3 > 0$, the parameter values in the set*

$$(7) \quad \varphi_H = \{(\mu_2, \mu_1) : \mu_1 = \pm(\mu_3/3)^{3/2} \mp (\mu_3/3)^{1/2} \mu_2, \quad \mu_2 < -\mu_3\},$$

represent Andronov-Hopf bifurcation points of codimension one for the central equilibrium point \mathbf{x}_C , see Lemma 2(c).

(c) *The set defined in (7) determines a symmetric pair of straight half lines emanating from two points corresponding to Bogdanov-Takens bifurcation points, namely*

$$(8) \quad BT_{\pm} \equiv \left(-\mu_3, \pm 2(\mu_3/3)^{3/2}\right).$$

Proof. Statement (a) is a direct consequence of the equations

$$x^3 + \mu_2 x + \mu_1 = 0, \quad \mu_2 + 3x^2 = 0,$$

to be fulfilled for any non-hyperbolic equilibrium $(x, 0)$ at a saddle-node bifurcation.

Let $(\tilde{x}, 0)$ an equilibrium point of system (3). Considering the Jacobian matrix J given in (4), then $J(\tilde{x}, 0)$ has two purely imaginary eigenvalues when taking $\mu_3 > 0$, the value \tilde{x} satisfies $\tilde{x} = \pm\sqrt{\mu_3/3}$ with $\mu_2 < -\mu_3 < 0$, because then $\mu_2 + 3\tilde{x}^2 < 0$. The last inequality is fulfilled only for the equilibrium point \mathbf{x}_C , see Lemma 2(c). Since $(\tilde{x}, 0)$ is an equilibrium point we have

$$\mu_1 + \mu_2 \left(\pm\sqrt{\mu_3/3}\right) + \left(\pm\sqrt{\mu_3/3}\right)^3 = 0,$$

and statement (b) follows. To show statement (c) is sufficient to consider the equations $\text{trace}(J(\tilde{x}, 0)) = \det(J(\tilde{x}, 0)) = 0$. \square

3. GLOBAL BIFURCATIONS

In this section we will complete the bifurcation analysis of system (3). We will write the system as a perturbed Hamiltonian to which the Melnikov theory can be applied. This can be done in different ways, as indicated in the next result. The possibility of resorting to one of the two next reparametrization forms will be helpful later.

Proposition 4. *System (3) can be written as two different perturbed Hamiltonian systems, as follows.*

(a) *Taking*

$$(9) \quad \mu_1 = \varepsilon^4 \nu_1, \quad \mu_2 = -\varepsilon^2 \nu_2, \quad \mu_3 = \varepsilon^2 \nu_3,$$

the system can be rewritten as

$$(10) \quad \begin{aligned} \dot{x} &= y, \\ \dot{y} &= -\nu_2 x + x^3 + \varepsilon (\nu_1 + \nu_3 y - 3x^2 y), \end{aligned}$$

which for $\varepsilon = 0$ corresponds to the Hamiltonian

$$(11) \quad H_1(x, y) = \frac{y^2}{2} + \nu_2 \frac{x^2}{2} - \frac{x^4}{4}.$$

(b) *Taking*

$$(12) \quad \mu_1 = \varepsilon^3 \nu_1, \quad \mu_2 = -\varepsilon^2 \nu_2, \quad \mu_3 = \varepsilon^2 \nu_3,$$

the system can be rewritten as

$$(13) \quad \begin{aligned} \dot{x} &= y, \\ \dot{y} &= \nu_1 - \nu_2 x + x^3 + \varepsilon (\nu_3 y - 3x^2 y), \end{aligned}$$

which for $\varepsilon = 0$ corresponds to the Hamiltonian

$$(14) \quad H_2(x, y) = \frac{y^2}{2} - \nu_1 x + \nu_2 \frac{x^2}{2} - \frac{x^4}{4}.$$

Proof. The blow-up transformation $x_1 = (1/\varepsilon)x$, $y_1 = (1/\varepsilon^2)y$, and $\tilde{t} = \varepsilon t$, allows to rewrite system (3) as

$$x'_1 = y_1, \quad y'_1 = x_1^3 + \frac{\mu_2}{\varepsilon^2} x_1 + \frac{\mu_1}{\varepsilon^3} + \frac{\mu_3}{\varepsilon} y_1 - 3\varepsilon x_1^2 y_1,$$

where the prime denotes derivatives with respect to the new time \tilde{t} . Now, using (9) and (12), after some elementary algebra we obtain systems (10) and (13), respectively. \square

The phase portrait for the unperturbed Hamiltonian systems (10) and (14) are shown in Figure 1. Note that when $\nu_1 = 0$ we obtain $H_1(x, y) = H_2(x, y)$, and so in that case it is sufficient to study the properties of the Hamiltonian H_1 .

Now, we will consider the heteroclinic connections of unperturbed Hamiltonian system (11). The Hamiltonian has a pair of heteroclinic connections $\Gamma_{\pm}(t) = (x(t), \pm y(t))$, parameterized by

$$(15) \quad \begin{aligned} x(t) &= \sqrt{\nu_2} \tanh\left(\sqrt{\nu_2/2}t\right), \\ y(t) &= \frac{\nu_2}{\sqrt{2}} \operatorname{sech}^2\left(\sqrt{\nu_2/2}t\right), \end{aligned}$$

where $-\infty < t < \infty$ and $\nu_2 > 0$. In the next result, we compute the Melnikov function along the heteroclinic connection Γ_+ for the unperturbed Hamiltonian system (10), and by using (9), we obtain the approximate bifurcation curves for heteroclinic connections for system (3).

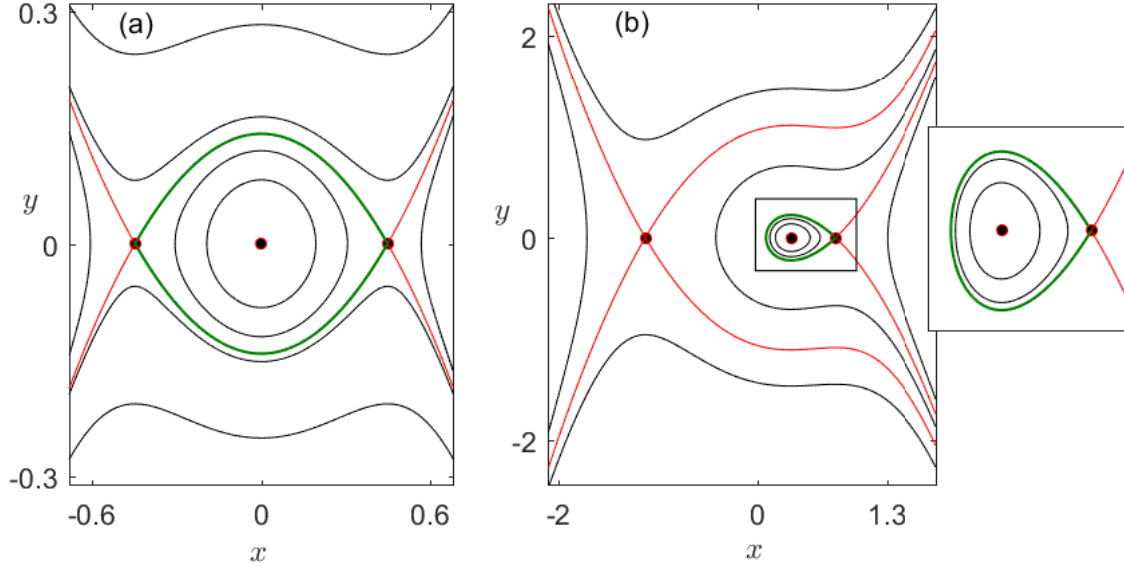


FIGURE 1. (a) Phase portrait of unperturbed Hamiltonian system (10) with $\nu_2 = 0.2$. We show in green the two heteroclinic orbits, while the non-closing stable and unstable manifolds of the saddle points are shown in red. (b) Phase portrait of unperturbed Hamiltonian system (13) with $\nu_1 = 0.3$ and $\nu_2 = 1$. We draw in green the homoclinic orbit, the stable and unstable manifolds of the saddle points are shown in red.

Proposition 5. *If we consider perturbed Hamiltonian system (10) and $\bar{\nu} = (\nu_1, \nu_2, \nu_3)$ with $\nu_2 > 0$ and $\nu_2^2/4 < \nu_2^3/27$ (see Lemma 2(c)) then the Melnikov function along of the heteroclinic connection Γ_{\pm} is given by*

$$(16) \quad M_{ht}(\bar{\nu}) = \frac{2}{15} \sqrt{\nu_2} \left(15\nu_1 + 5\sqrt{2}\nu_2\nu_3 - 3\sqrt{2}\nu_2^2 \right).$$

Proof. The system can be written as

$$(\dot{x}, \dot{y})^T = f(x, y) + \varepsilon g(x, y),$$

where $f(x, y) = (y, -\nu_2 x + x^3)^T$ and $g(x, y) = (0, \nu_1 + \nu_3 y - 3x^2 y)^T$. Thus, we have $f \wedge g = y(\nu_1 + \nu_3 y - 3x^2 y)$. Accordingly, the Melnikov function is defined by

$$\begin{aligned} M_{ht}(\bar{\nu}) &= \int_{-\infty}^{\infty} f(x(t), \pm y(t)) \wedge g(x(t), \pm y(t)) dt = \\ &= \int_{-\infty}^{\infty} \pm y(t) [\nu_1 \pm (\nu_3 - 3x^2(t))y(t)] dt, \end{aligned}$$

where $x(t)$ and $y(t)$ are defined as in (15). After a direct computation we obtain (16). \square

By using the Melnikov theory and by fixing one parameter of system (3), we can give an approximation of the heteroclinic connection curves in the remaining parameters plane.

Proposition 6. *Consider system (3) with $\mu_3 > 0$ sufficiently small and the parametric plane (μ_2, μ_1) . Then the system has a unique hyperbolic heteroclinic connection in a neighborhood of the curve*

$$(17) \quad \varphi_{ht} = \{(\mu_2, \mu_1) \in \mathbb{R}^2 : \mu_1 = \pm \frac{\sqrt{2}}{15} \mu_2 (3\mu_2 + 5\mu_3), \quad \mu_2 \neq -5\mu_3/3\}.$$

Proof. Fixing $\nu_3 = 1$ in the Melnikov function given in (16), and imposing the condition $M_{ht}(\nu_1, \nu_2) = 0$, we obtain

$$\nu_1 = \frac{\sqrt{2}}{15} \nu_2 (3\nu_2 - 5).$$

From (9) we get $\varepsilon = \sqrt{\mu_3}$, $\mu_1 = \mu_3^2 \nu_1$, and $\mu_2 = -\mu_3 \nu_2$, so that

$$\mu_1 = \mu_3^2 \nu_1 = -\mu_3^2 \frac{\sqrt{2}}{15} \frac{\mu_2}{\mu_3} \left(3 \left(-\frac{\mu_2}{\mu_3} \right) - 5 \right),$$

and the conclusion follows. \square

When $\mu_1 = 0$ and $\mu_3 > 0$ on the parameter plane (μ_2, μ_1) , we obtain the point of double heteroclinic connections

$$(18) \quad DHT \equiv (-5\mu_3/3, 0).$$

We recall that Schecter's points are co-dimension two points defined by the intersection of a saddle-node curve and a homoclinic or heteroclinic curve, for more details see [32]. Taking the intersection points of the saddle-node bifurcation curve and the heteroclinic curves given in (6) and (17) respectively, we obtain a first-order approximation of Schecter's points of the system. Since the system is symmetric with respect to the parameter μ_1 , the system has four Schecter's points (see Figure 3), these points are

$$(19) \quad \begin{aligned} S_1^\pm &\equiv \rho_1 \left((5/27), \mp (5\sqrt{10}/729) \left(\sqrt{18\mu_3 + 5} + \sqrt{5} \right) \right), \\ S_2^\pm &\equiv \rho_2 \left((5/27), \pm (5\sqrt{10}/729) \left(\sqrt{18\mu_3 + 5} - \sqrt{5} \right) \right), \end{aligned}$$

where

$$\rho_1 = \left(9\mu_3 + 5 - \sqrt{5}\sqrt{18\mu_3 + 5} \right), \quad \rho_2 = \left(\sqrt{5}\sqrt{18\mu_3 + 5} - 9\mu_3 - 5 \right).$$

Now, by using the homoclinic connection of Hamiltonian system (14), we compute the associated Melnikov function for system (3) when $\nu_3 = 1$.

Proposition 7. *If we consider system (13) and $\bar{\nu} = (\nu_1, \nu_2, \nu_3)$ with $\nu_1 > 0$, $\nu_2 > 0$ and $\nu_3 = 1$, then the Melnikov function associated to the homoclinic orbit with connection point $(0, s_R)$, it is given by*

$$(20) \quad M(\bar{\nu}) = \sqrt{2} \frac{\cosh^2(\theta)}{\cosh^2(\theta) + 2} (F_1(\theta) + \nu_2 F_2(\theta)),$$

where

$$(21) \quad \begin{aligned} F_1(\theta) &= 720\theta - 320 \sinh \theta + 240\theta \cosh^3 \theta - 320 \cosh^2 \theta \sinh \theta - \\ &\quad - 80 \cosh^4 \theta \sinh \theta + 480\theta \cosh \theta, \\ F_2(\theta) &= 1440\theta \cosh \theta - 768 \sinh \theta - \cosh^3 \theta - 1344 \cosh^2 \theta \sinh \theta - \\ &\quad - 48 \cosh^4 \theta \sinh \theta \end{aligned}$$

and $0 < \theta < \infty$, with

$$\cosh \theta = \frac{2s}{\omega}, \quad \omega^2 = 2(\nu_2 - s_R^2) > 0, \quad \nu_1 = \nu_2 s_R - s_R^3,$$

being s_R the biggest positive root of the equation $\nu_1 - \nu_2 x + x^3 = 0$, see Figure 2.

Proof. We consider the unperturbed Hamiltonian system given in (13) with $\nu_2 > 0$. From Lemma 2(c), the system has 3 equilibrium points $\mathbf{x}_i = (s_i, 0)$, where \mathbf{x}_L and \mathbf{x}_R are saddle points and \mathbf{x}_C is a focus or node and

$$s_L < s_C < s_R, \quad s_L + s_C + s_R = 0, \quad s_L s_C s_R = -\nu_1.$$

We study only the case $\nu_1 > 0$, for the case $\nu_1 < 0$ is analogous.

System (13) can be written as

$$(\dot{x}, \dot{y})^T = f(x, y) + \varepsilon g(x, y).$$

Now, assuming $\nu_1 > 0$, by Green's Theorem, the homoclinic Melnikov function of the system can be rewritten as

$$M_h(\bar{\nu}) = \int \int_{D(\nu_1, \nu_2)} \left(\frac{-\partial g(x, y)}{\partial y} \right) dA,$$

where D is the region bounded by the homoclinic orbit which joins the equilibrium point $(s_R, 0)$ to itself. By fixing $\nu_3 = 1$ (that is $\mu_3 > 0$), and taking $p(x) = \nu_1 - \nu_2 x + x^3$, we get $p(s_R) = \nu_1 - \nu_2 s_R + s_R^3 = 0$, that is

$$(22) \quad \nu_1 = s_R(\nu_2 - s_R^2),$$

and so $\nu_2 - s_R^2 > 0$. Taking the auxiliary function

$$q(x) = \int_0^x p(x) dx = \nu_1 x - \nu_2 \frac{x^2}{2} + \frac{x^4}{4},$$

and using (14), the homoclinic loop is given by the points $(x, y_s^\pm(x))$ where $\bar{x} \leq x \leq s_R$,

$$y_s^\pm(x) = \pm \sqrt{2} \sqrt{q(x) - q(s_R)},$$

and $y_s^\pm(\bar{x}) = y_s^\pm(s_R) = 0$, see Figure 2. Now, the Melnikov function is thanks to the symmetry of the loop

$$\begin{aligned} M_h(\bar{\nu}) &= 2 \int_{\bar{x}}^{s_R} (3x^2 - 1) dx \int_0^{y_s^+(x)} dy = \\ &= \sqrt{2} \int_{\bar{x}}^{s_R} (3x^2 - 1)(s_R - x) \sqrt{(x + s_R)^2 - 2(\nu_2 - s_R^2)} dx = \\ &= \sqrt{2} \int_{\bar{x}}^{s_R} (3x^2 - 1)(s_R - x) \sqrt{(x + s_R)^2 - \omega^2} dx, \end{aligned}$$

where from (22) $\omega^2 = 2(\nu_2 - s_R^2)$, and we have used that

$$q(x) - q(s_R) = \frac{1}{4}(x - s_R)^2 [(x + s_R)^2 - \omega^2].$$

Taking the change of variable

$$x + s_R = \omega \cosh \theta,$$

and noting that $q(s_R) - q(\bar{x}) = 0$ we see that $\bar{x} + s_R = \omega$, which corresponds to $\theta = 0$, while for $x = s_R$ the corresponding values of $\theta = \theta_{s_R}$ satisfy $\cosh \theta_{s_R} = 2s_R/\omega$, or also $\omega^2 \cosh^2 \theta_{s_R} = 4s_R^2$, that is $(s_R^2 + \nu_2) \cosh^2 \theta_{s_R} = 2s_R^2$, and so we get

$$s_R^2 = \frac{\cosh^2 \theta_{s_R}}{2 + \cosh^2 \theta_{s_R}} \nu_2.$$

Now we arrived to

$$M_h(\bar{\nu}) = \sqrt{2}\omega^2 \int_0^{\theta_{s_R}} (1 - 3(\omega \cosh \theta - s_R)^2)(2s_R - \omega \cosh \theta) \sinh^2 \theta d\theta,$$

and after some computations, we obtain (20) and (21), where θ_{s_R} has been simplified to θ . \square

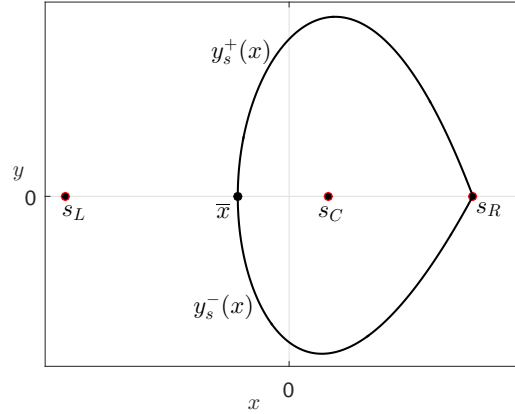


FIGURE 2. Homoclinic orbit which joins the saddle equilibrium point $(s_R, 0)$ to itself.

As a direct consequence of the above result, we give an analytical approximation of the bifurcation curves for homoclinic connections of system (3).

Proposition 8. *Consider system (3) with $\mu_3 > 0$ sufficiently small and the parametric plane (μ_2, μ_1) . Then the system has a unique homoclinic orbit in a neighborhood of the curve*

$$(23) \quad \varphi_h = \{(\mu_2, \mu_1) \in \mathbb{R}^2 : \mu_2 = -\mu_3 \nu_2(\theta), \quad \mu_1 = \pm \mu_3^{3/2} \nu_1(\theta), \quad 0 < \theta < \infty\},$$

where

$$(24) \quad \nu_2(\theta) = \frac{10(\cosh 2\theta + 5)(9 \sinh \theta + \sinh 3\theta - 12\theta \cosh \theta)}{3(370 \sinh \theta + 115 \sinh 3\theta + \sinh 5\theta - 60\theta(11 \cosh \theta + \cosh 3\theta))},$$

$$\nu_1(\theta) = \nu_2(\theta) s - s^3, \quad s^2 = \frac{\cosh^2 \theta}{2 + \cosh^2 \theta} \nu_2(\theta).$$

Moreover, for the points $(\mu_2(\theta), \mu_1(\theta))$ at the curve φ_h we have.

$$\lim_{\theta \rightarrow 0^+} (\mu_2, \mu_1) = (-\mu_3, \pm 2/3 \sqrt{\mu_3^3/3}), \quad \lim_{\theta \rightarrow \infty} (\mu_2, \mu_1) = (-5\mu_3/3, 0).$$

Proof. The Melnikov function given in (20)-(21) vanishes at the points $(\nu_1(\theta), \nu_2(\theta))$ defined in (24). Taking $\nu_3 = 1$ in (12) we obtain $\mu_1 = \mu_3^{3/2} \nu_1$ and $\mu_2 = -\mu_3 \nu_2$, and after some computations the conclusion follows. \square

Remark 9. Note that from the previous result we obtain the two points

$$\lim_{\theta \rightarrow 0^+} (\mu_2, \mu_1) \equiv BT, \quad \lim_{\theta \rightarrow \infty} (\mu_2, \mu_1) \equiv DHT,$$

where the points *BT* and *DHT* are given in (8) and (18) respectively.

In Figure 3, the complete bifurcation set of system (3) is shown. Figures 4 and 5 give the different phase portrait in the labeled parameter regions, where in these figures we show the different configurations of the phase portrait of the system. In Figure 4, since the homoclinic Melnikov function is positive, we can guarantee that there is no change on the relative position of the stable and unstable manifolds of each saddle points.

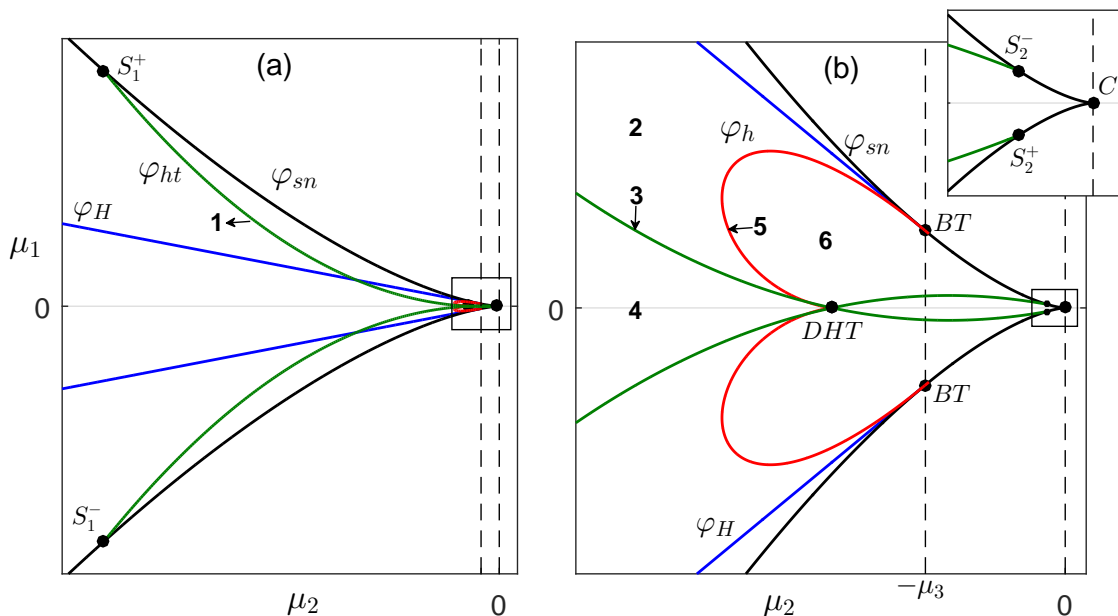


FIGURE 3. The bifurcation diagram of system (3), taking $\mu_3 > 0$ sufficiently small.

Remark 10. Note that considering the function ν_2 defined in (24), and after some algebra, we obtain that finding the minimum of the function ν_2 is equivalent to finding the zeros of the function

$$(25) \quad h_1(x) = 2x(26 \cosh 2x + \cosh 4x + 33) - 5(10 \sinh 2x + \sinh 4x),$$

where $h_1(0) = 0$, $h_1(1) < 0$ and $h_1(2) > 0$, see Figure 6(c). Thus at $\theta^* \approx 1.8630981$ the function ν_2 has a minimum given by $\nu_2(\theta^*) \approx 2.454887$ (see Figure 6(b)), so that

$$-\frac{5}{2}\mu_3 < -\nu_2(\theta^*)\mu_3 < -\frac{5}{3}\mu_3.$$

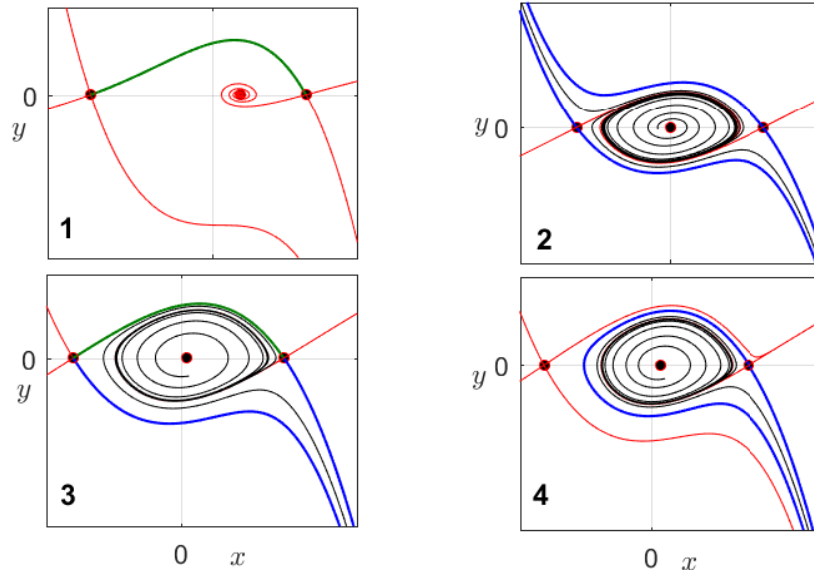


FIGURE 4. Phase portrait of system (3) in the parameter regions labeled with **1, 2, 3** and **4** in Figure 3. The thick lines are the boundary of the basin of attraction of a limit cycle, such boundary is formed by some stable and unstable manifolds of the saddle points. The green lines are the heteroclinic connections.

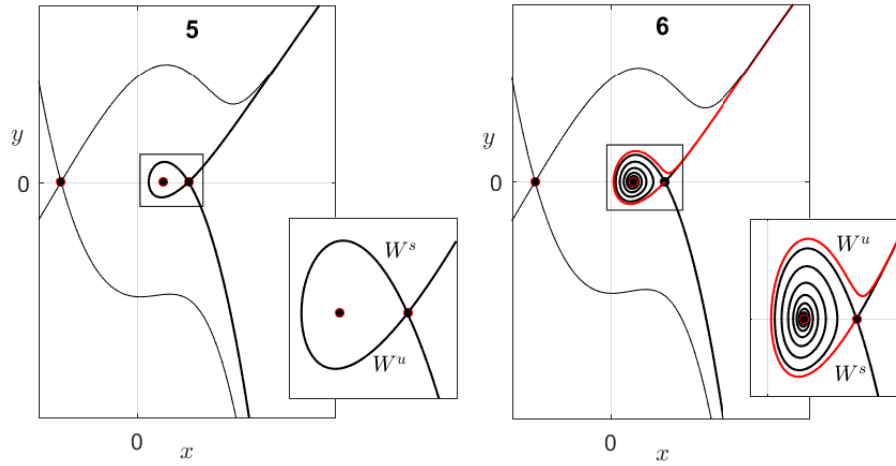


FIGURE 5. Phase portrait of system (3) in the parameter regions labeled with **5** and **6** in Figure 3. The stable and unstable manifolds of the saddle points.

Now, if we consider system (3) with $\mu_3 > 0$ sufficiently small, $\mu_2 < -(5/2)\mu_3$ and μ_1 such that

$$|\mu_1| < \left(\frac{\mu_3}{3}\right)^{3/2} - \left(\frac{\mu_3}{3}\right)^{1/2} \mu_2,$$

then the system has a stable limit cycle, see Figure 6(a). This assertion is a direct consequence of (7) and Poincaré-Bendixson Theorem (see for instance [35]), since

the sign of the Melnikov function guarantees the existence of a compact positive invariant set with only one unstable equilibrium point in its interior.

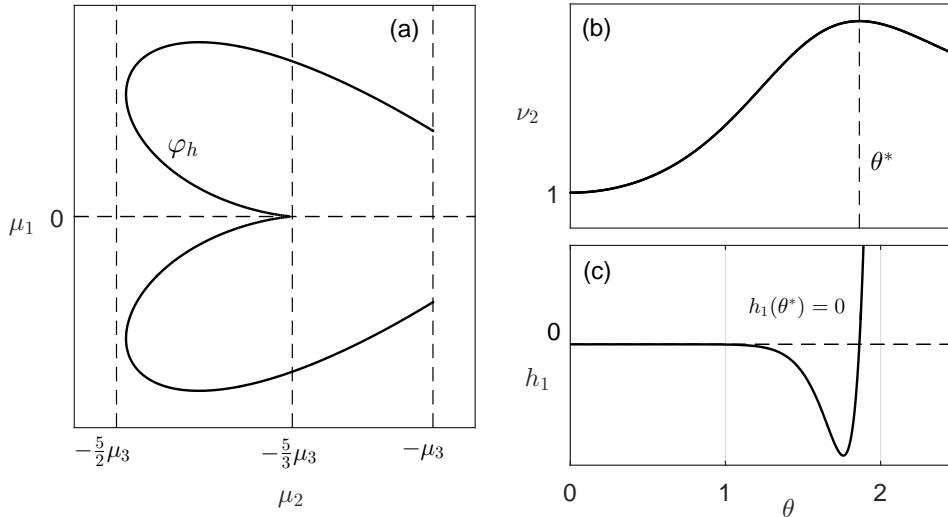


FIGURE 6. (a) The parametric curve defined in (23) on the plane of parameters (μ_2, μ_1) . (b) The function $\nu_2(\theta)$ defined in (24). (c) The function $h(\theta)$ defined in (25).

Just to illustrate the quality of the above analytical predictions for the homoclinic connection bifurcation curve, by using the shooting method (see for instance [31]) and taking $\mu_3 = 0.1$, we show in Figure 7, the numerical continuation curve for the homoclinic orbit of system (3), and in red the analytic approximation curve given by (23). As observed, there is a great similarity between the two approaches, and in general we can conclude that the above analytical predictions are really useful in getting a global view of the actual bifurcation set.

4. APPLICATION TO 3D CANONICAL MEMRISTOR OSCILLATOR

As one of the possible applications of the above study, in this section we will show the existence of a topological sphere completely foliated by periodic orbits for a 3D canonical memristor oscillator, when the flux-charge characteristics of the memristor is a monotone cubic polynomial. The existence of this sphere was reported numerically in [29, 25].

We start by considering the modeling of an elementary oscillator endowed with one flux-controlled memristor M , see Figure 8 and [22]. In the shown circuit the values of L and C for the impedance and capacitance are positive constants, while the resistor has a negative value $-R$. From Kirchoff's laws we see that

$$\begin{aligned} i_R(\tau) - i_L(\tau) &= 0, \\ i_L(\tau) - i_C(\tau) - i_M(\tau) &= 0, \\ -v_R(\tau) + v_L(\tau) + v_C(\tau) &= 0, \\ v_C(\tau) - v_M(\tau) &= 0, \end{aligned}$$

where v, i stand for the voltage and current, respectively, across the corresponding element of the circuit as indicated by the subscript.

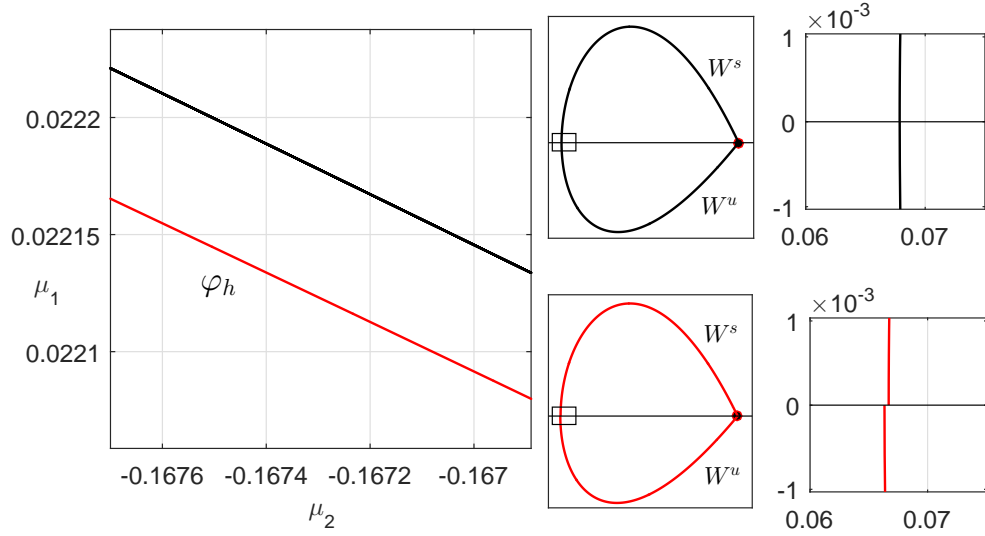


FIGURE 7. System (3) with $\mu_3 = 0.1$. In black (left panel), the numerical continuation curve in the parameter plane (μ_2, μ_1) , and by using points of the curve, in black (right panel) the numerical computation of the stable and unstable manifold for a saddle point of the system. In red (left panel), the analytic approximation curve given by (23), and by using points of the curve, in red (right panel) the numerical computation of the stable and unstable manifolds for a saddle point of the system.

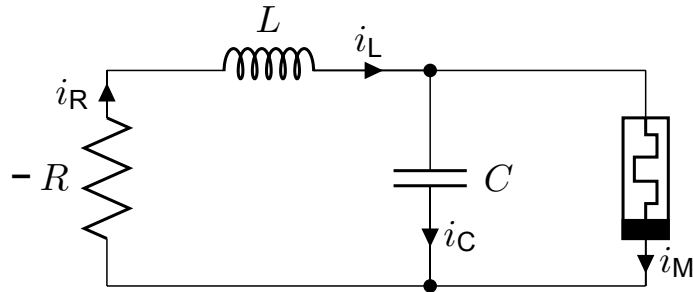


FIGURE 8. The canonical memristor oscillator [22]. Note that the the only active element in the circuit is the resistor with a negative resistance $-R$.

In Section 3.2 of [22], this circuit is proposed as a third-order canonical memristor oscillator but the notation is slightly different as follows. They take $i_1 = i_C$, $i_3 = i_L = i_R$, $i = i_M$, $v_1 = v_C = v_M$, $v_3 = v_L$, $v_4 = v_R$, $\varphi_1 = \varphi_C$, $\varphi_3 = \varphi_L$, $\varphi_4 = \varphi_R$ and $\varphi = \varphi_M$. Thus, they write the two equations

$$i_1 = i_3 - i, \quad v_3 = v_4 - v_1,$$

and, after integrating respect to time, they arrive to

$$(26) \quad q_1 = q_3 - q(\varphi), \quad \varphi_3 = \varphi_4 - \varphi_1,$$

where $q(\varphi)$ stands for the nonlinear flux-charge characteristics of the flux-controlled memristor. Solving now for (q_3, φ_4) and taking into account that $\varphi_1 = \varphi$ since

$v_1 = v_M$, it is immediate to obtain

$$q_3 = q_1 + q(\varphi), \quad \varphi_4 = \varphi + \varphi_3,$$

so that authors conclude that a good choice for independent variables is the triple $(q_1, \varphi_3, \varphi)$, that is, the charge of capacitor C , the flux of the inductor L and the flux of the memristor, respectively. Accordingly, by taking derivatives in (26), the following set of differential equations is proposed,

$$(27) \quad \begin{aligned} C\dot{v}_1 &= i_3 - W(\varphi)v_1, \\ L\dot{i}_3 &= Ri_3 - v_1, \\ \dot{\varphi} &= v_1, \end{aligned}$$

where $\dot{q}_1 = i_1 = C\dot{v}_1$, $\dot{q}_3 = i_3$, $\dot{\varphi}_4 = v_4 = Ri_3$ and

$$W(\varphi) = \frac{dq}{d\varphi}.$$

Finally, they rewrite the system as follows,

$$(28) \quad \begin{aligned} \dot{x} &= \alpha(y - W(z)x), \\ \dot{y} &= -\xi x + \beta y, \\ \dot{z} &= x, \end{aligned}$$

where $x = v_1$, $y = i_3$, $z = \varphi$, and the parameters used are $\alpha = 1/C$, $\xi = 1/L$, and $\beta = R/L$, so that, $\alpha, \xi, \beta > 0$. An important observation is that the parameter α is not essential so that it can be removed with the change of variables and parameters

$$(29) \quad \begin{aligned} \tilde{x} &= x, \quad \tilde{y} = \alpha y, \quad \tilde{z} = z, \quad \tilde{\xi} = \alpha \xi, \\ \tilde{a} &= \alpha a, \quad \tilde{b} = \alpha b, \quad \tilde{W} = \alpha W, \end{aligned}$$

to be assumed in the sequel, omitting also tildes to alleviate the notation. Therefore, we need to study the system

$$(30) \quad \begin{aligned} \dot{x} &= -W(z)x + y, \\ \dot{y} &= -\xi x + \beta y, \\ \dot{z} &= x, \end{aligned}$$

where $W(z) = q'(z) = 3z^2 + 2az + b$, and

$$(31) \quad q(z) = z^3 + az^2 + bz,$$

with $a^2 - 3b < 0$, which assumes that the memristor is passive ($q'(z) > 0$).

System (30) belongs to a more general class of systems whose reduction is possible thanks to the existence of a first integral, as shown in the Appendix. Like other models of memristor oscillators, system (30) has some special feature. For instance, it has a continuum of equilibria on the z -axis. Furthermore, the Jacobian matrix at any of these points has a zero eigenvalue.

Taking the parameters $a_{11} = -1$, $a_{12} = 1$, $a_{21} = -\xi$ and $a_{22} = \beta$ in Proposition 16 of the appendix, we obtain that for all $h \in \mathbb{R}$, system (30) has an invariant manifold S_h defined by

$$(32) \quad S_h = \{(x, y, z) \in \mathbb{R}^3 : -\beta x + y - \beta z^3 - a\beta z^2 + (\xi - b\beta)z = h\}.$$

Moreover, assuming $c = 1$ in Corollary 18 of the appendix, we obtain that on each invariant manifold S_h , the system is topologically equivalent to the Liénard system

$$(33) \quad \begin{aligned} \dot{x} &= y - x^3 - x^2 - (b - \beta)x, \\ \dot{y} &= \beta x^3 + a\beta x^2 + (b\beta - \xi)x + h. \end{aligned}$$

In Figure 9, we show the invariant manifold (32) corresponding to $h = 0.3$ and the set of parameters $\xi = 100$, $a = b = 1$, $\beta = 5$, along with the phase space of the equivalent Liénard system (33). From Proposition 19(a), the system can be

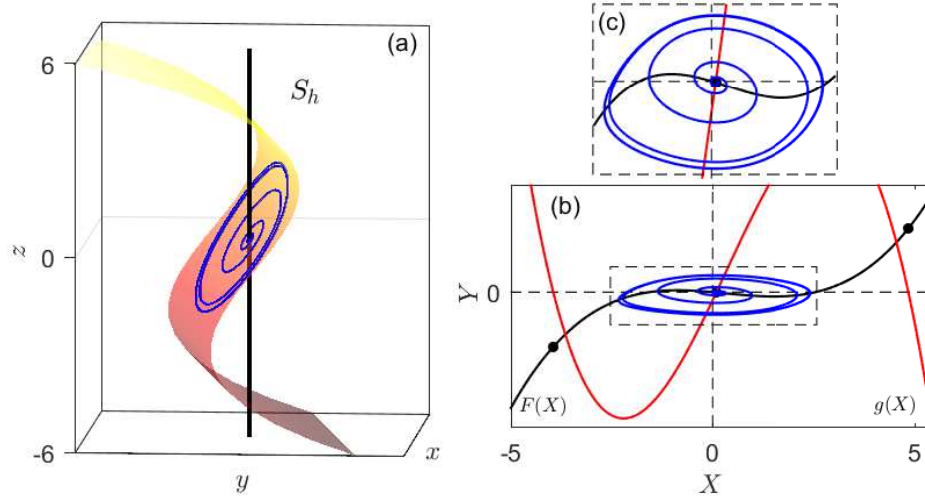


FIGURE 9. (a) The invariant manifold (32) corresponding to the set of parameters $\xi = 100$, $a = b = 1$, $\beta = 5$ and $h = 0.3$ is shown. In black the infinite number of equilibrium points of the system and in blue a periodic orbit of the system contained in the invariant manifold. (b) The phase plane of the equivalent Liénard system (33) corresponding to the set parameters given in (a) showing a limit cycle in blue, in red the function $g(X)$ and the function $F(X)$ in black. (c) A zoom of figure (b) is shown.

rewritten as

$$(34) \quad \dot{x} = y, \quad \dot{y} = \mu_1 + \mu_2 x + \mu_3 y + x^3 - 3x^2 y,$$

where the new parameter are

$$(35) \quad \begin{aligned} \mu_1 &= \frac{1}{27\beta^{5/2}}(27h + 9a\xi + 2a^3\beta - 9ab\beta), \\ \mu_2 &= \frac{1}{3\beta^2}(\beta(3b - a^2) - 3\xi), \quad \mu_3 = \frac{1}{3\beta}(a^2 - 3b + 3\beta). \end{aligned}$$

From Remark 10, for $\mu_3 > 0$ sufficiently small, we have that for all $\mu_2 < -(5/2)\mu_3 < 0$ and μ_1 such that

$$(36) \quad |\mu_1| < \left(\frac{\mu_3}{3}\right)^{3/2} - \left(\frac{\mu_3}{3}\right)^{3/2} \mu_2,$$

the system has a stable limit cycle. Therefore, we can give the following result in terms of the parameter h , which is associated with the invariant manifolds S_h of 3D

system (46). This result guarantees the existence of a topological sphere in the 3D phase-space completely foliated by periodic orbits.

Proposition 11. *Consider system (30) with $\beta, \xi > 0$, the function q defined as in (31), $a^2 - 3b < 0$ and*

$$(37) \quad a^2 - 3b + 3\beta > 0$$

sufficiently small. Additionally, suppose that the following inequalities hold

$$(38) \quad \begin{aligned} 0 < 3b - a^2 < 3\xi/\beta, \\ \beta(3b - a^2) - 3\xi < (5/2)(3b - a^2 - 3\beta)\beta < 0. \end{aligned}$$

Then for all $h \in \mathbb{R}$ with

$$-\frac{A}{27} < h < \frac{B}{27},$$

where

$$(39) \quad \begin{aligned} A &= (4a^2\beta + 3\beta^2 - 12b\beta + 9\xi) \sqrt{a^2 - 3b + 3\beta} + 9a\xi + 2a^3\beta - 9ab\beta, \\ B &= (4a^2\beta + 3\beta^2 - 12b\beta + 9\xi) \sqrt{a^2 - 3b + 3\beta} - 9a\xi - 2a^3\beta + 9ab\beta, \end{aligned}$$

the system has a stable periodic orbit. Moreover, there exist a topological sphere Ω (see Figure 10) foliated by such periodic orbits.

Proof. From Remark 10, and after substituting the values of μ_1, μ_2 and μ_3 given in (35), we obtain the inequalities (37)-(38). Now, from (36) we obtain $|\mu_1| < (1/3)(\mu_3/3)^{1/2}(\mu_3 - 3\mu_2)$, so that $\mu_3 - 3\mu_2 > 0$, since from hypotheses we have $\mu_2 < -(5/2)\mu_3 < 0$. Now after some algebra we obtain

$$|27h + 9a\xi + 2a^3\beta - 9ab\beta| < (4a^2\beta + 3\beta^2 - 12b\beta + 9\xi) \sqrt{a^2 - 3b + 3\beta}.$$

Taking into account the absolute value, and grouping terms, we obtain the values of A and B defined in (39). Finally, from Remark 10 system (30) has a stable periodic orbit on each S_h defined in (32), so varying the parameter h , we obtain a sphere foliated by such periodic orbits. \square

5. FALSE HIDDEN ATTRACTORS IN MEMRISTOR-BASED AUTONOMOUS DUFFING OSCILLATORS

An attractor is called a hidden attractor if its basin of attraction does not intersect any neighborhood of equilibria; otherwise, it is called a self-excited attractor, for more details see [26, 27]. Recently in [33, 34, 19] it was reported the existence of an infinite number of hidden attractors in a memristor-based autonomous Duffing oscillators, whose memristance function is a cubic polynomial. Here, by using a similar approach to the followed in the previous section, we will show that such hidden attractors are not possible, so that the numerical simulations included in [33, 34, 19] are misleading.

The quoted memristor based autonomous Duffing oscillator is modeled by the dynamical system

$$(40) \quad \begin{aligned} \dot{x} &= y, \\ \dot{y} &= z, \\ \dot{z} &= -\alpha z - M(x)y, \end{aligned}$$

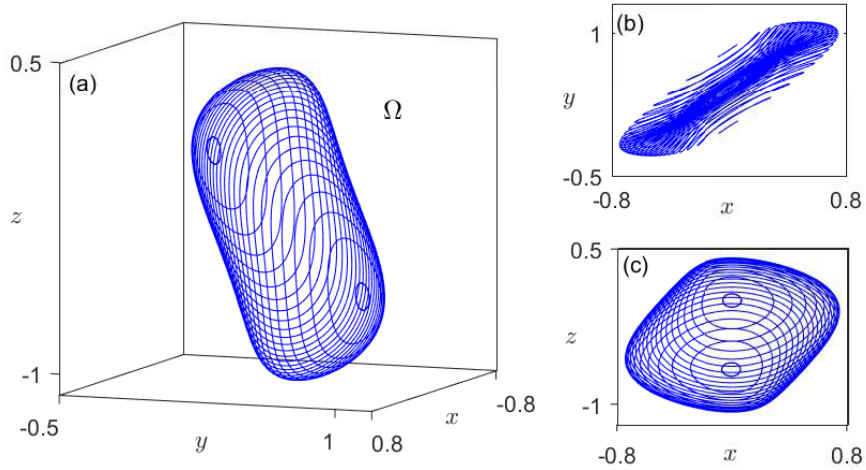


FIGURE 10. Using (62) on each invariant manifold S_h defined in (32), some slices of the surface Ω given by Proposition 11 for system (30) with parameters $a = 1, b = 4.8, \beta = 5$ and $\xi = 80$ are shown. For this set of parameters we get $\mu_3 = 0.106 > 0$, $\mu_2 = -2.3 < -(5/2)\mu_3$, $A = 1180.1$ and $B = 152.2$.

where the memristance function M (possibly discontinuous) is defined as

$$(41) \quad M(x) = \frac{d\phi(x)}{dx}$$

and ϕ is a continuous function. System (40) has a continuum of equilibria, since any point of the x -axis is an equilibrium point. In the next result, we show that even system (40) does not belong to the family (46) of the appendix, the system also has the property of possessing an infinite number of invariant manifolds.

Proposition 12. *Consider system (40) with the function M defined as in (41). For any $h \in \mathbb{R}$ the set*

$$(42) \quad S_h = \{(x, y, z) \in \mathbb{R}^3 : H(x, y, z) = h\}$$

is an invariant manifold for the system, where we have introduced the continuous function

$$(43) \quad H(x, y, z) = \phi(x) + \alpha y + z.$$

Therefore, the system has an infinite number of invariant manifolds foliating the whole \mathbb{R}^3 , and so the dynamics is essentially two-dimensional.

Proof. Taking H as in (43), define for any solution $(x(\tau), y(\tau), z(\tau))$ of (40) the auxiliary continuous function

$$h(\tau) = H(x(\tau), y(\tau), z(\tau))$$

Now, a direct computation gives, excepting the points of possible non-differentiability,

$$h'(\tau) = \frac{d\phi(x)}{dx} \dot{x} + \alpha \dot{y} + \dot{z} = M(x)y + \alpha z - \alpha z - M(x)y = 0.$$

Then h is piecewise constant along the orbits of (40), but as h is continuous by definition, it should be globally constant. In short, the level sets of H are invariant for the flow. \square

Now, by using the above result, we reduce the study of the dynamical behavior of the system, to the study of a planar system.

Proposition 13. *Consider system (40) with the function M defined as in (41). Then on each invariant set S_h defined in (42) the system is topologically equivalent to the planar system*

$$(44) \quad \begin{aligned} \dot{x} &= y, \\ \dot{y} &= -\phi(x) - \alpha y + h. \end{aligned}$$

Moreover, $(x(\tau), y(\tau)) \in \mathbb{R}^2$ is a solution of the above system if and only if $E_h(x(\tau), y(\tau))$ is a solution of system (40), where

$$(45) \quad E_h(X(\tau), Y(\tau)) = \begin{pmatrix} x(\tau) \\ y(\tau) \\ h - \phi(x(\tau)) - \alpha y(\tau) \end{pmatrix}$$

Proof. From Proposition 12 we can solve for z in the equation $H(x, y, z) = h$, and write

$$z = h - \phi(x) - \alpha y.$$

Replacing this expression into the first and second equation of (40) we obtain system (44). Suppose that $(x(\tau), y(\tau)) \in \mathbb{R}^2$ is a solution of system (44). Taking

$$z(\tau) = h - \alpha y(\tau) - \phi(x(\tau))$$

we obtain

$$\begin{aligned} \dot{z}(\tau) &= -\alpha \dot{y}(\tau) - \frac{d\phi(x(\tau))}{dx} \dot{x}(\tau) = -\alpha (h - \phi(x(\tau)) - \alpha y(\tau)) - M(x(\tau))y(\tau) = \\ &= -\alpha (z(\tau)) - M(x(\tau))y(\tau). \end{aligned}$$

and the proposition follows. \square

In the following result, we show that for $\alpha \neq 0$, the system does not have periodic solutions.

Proposition 14. *Consider system (44). The following statements hold.*

- (a) *For $\alpha = 0$ the system is Hamiltonian.*
- (b) *For $\alpha \neq 0$ the system does not have periodic solutions.*

Proof. The divergence of the system is $\Delta = -\alpha$. Then, when $\alpha = 0$ the system corresponds to the Hamiltonian

$$H(x, y) = \frac{y^2}{2} + \phi'(x).$$

For $\alpha \neq 0$ the divergence of system (44) does not change sign, thus from Bendixson's criterion [21], system (40) does not have periodic solutions. \square

Remark 15. *Note that as a consequence of proposition 13 and 14, the 3D system (40) system cannot have periodic orbits for any continuous function ϕ and $\alpha \neq 0$. However, when $\alpha = 0$ the system could have an infinite number of periodic orbits on each invariant set S_h defined in (42).*

Regarding [33, 34, 19] authors consider system (40) with the function $\phi(x) = \omega x + \beta x^3$ and the set of parameters $\alpha = 0.0001$, $\omega = 0.35$, $\beta = 0.85$. In both quoted references, authors reported the existence of an infinite number of stable periodic orbits coexisting with an infinite number of stable equilibria, by taking into account several numerical simulations, so concluding the existence of hidden attractors.

From Propositions 12 and 13, we obtain the invariant manifolds

$$S_h = \{(x, y, z) \in \mathbb{R}^3 : \omega x + \beta x^3 + \alpha y + z = h\},$$

and the planar system ruling the dynamics on each S_h given by

$$\dot{x} = y, \quad \dot{y} = -\omega x - \beta x^3 - \alpha y + h.$$

From Remark 15 we note that, the system cannot have periodic orbits, and so, the statement made in the quoted papers is clearly wrong, probably after giving too much credit to numerical simulations. This emphasizes the relevance of the approach followed in this work which allows to avoid misconceptions coming just from numerical simulations.

6. CONCLUSIONS

Motivated by the dynamical analysis of 3D memristor oscillators whose nonlinear characteristics is a cubic polynomial, and after showing that their dynamics is essentially two-dimensional, the need to consider a disregarded unfolding of the Bogdanov-Takens singularity naturally arose. The corresponding bifurcation set, including both local and global bifurcations has been described. While local bifurcations can be easily detected, the characterization of global bifurcations parameters curves is much more involved; only by resorting to Melnikov's theory it was possible to obtain such curves providing a complete description of the bifurcation set.

Regarding the considered 3D memristor oscillators, and by working within some parameters regions of the above bifurcation set, it has been possible to show rigorously the existence of multiple periodic orbits leading to a topological sphere.

When the same approach is applied to a different family of 3D memristor oscillators, it has been shown that the oscillations are not possible, contrarily to what had been recently claimed.

ACKNOWLEDGEMENTS

The first author is supported by Pontificia Universidad Javeriana Cali-Colombia. E. Freire and E. Ponce are partially supported by MINECO/FEDER grant MTM2015-65608-P and by the *Consejería de Economía, Innovación, Ciencia y Empleo de la Junta de Andalucía* under grant P12-FQM-1658.

REFERENCES

- [1] A. Amador, E. Freire, E. Ponce, and J. Ros. On discontinuous piecewise linear models for memristor oscillators. *International Journal of Bifurcation and Chaos*, 27(06):1730022, jun 2017.
- [2] H.J. De Blank, Y. Kuznetsov, M.J. Pekkér, and D.W.M. Veldman. Degenerate Bogdanov-Takens bifurcations in a one-dimensional transport model of a fusion plasma. *Physica D: Nonlinear Phenomena*, 331:13 – 26, 2016.
- [3] T.R. Blows and L.M. Perko. Bifurcation of limit cycles from centers and separatrix cycles of planar analytic systems. *SIAM Review*, 36(3):341376, 1994.

- [4] H. Chen and X. Chen. Dynamical analysis of a cubic liénard system with global parameters. *Nonlinearity*, 28(10):35353562, Apr 2015.
- [5] H. Chen and X. Chen. Dynamical analysis of a cubic liénard system with global parameters (ii). *Nonlinearity*, 29(6):1798, 2016.
- [6] H. Chen and X. Chen. Global phase portrait of a degenerate bogdanov-takens system with symmetry II. *Discrete & Continuous Dynamical Systems-B*, 23(10):4141–4170, 2018.
- [7] H. Chen, X. Chen, and J. Xie. Global phase portrait of a degenerate bogdanov-takens system with symmetry. *Discrete & Continuous Dynamical Systems-B*, 22(4):1273–1293, 2017.
- [8] G. Dangelmayr and J. Guckenheimer. On a four parameter family of planar vector fields. *Archive for Rational Mechanics and Analysis*, 97(4):321352, 1987.
- [9] A. Dhooge, W. Govaerts, Y. Kuznetsov, H.G.E. Meijer, and B. Sautois. New features of the software matcont for bifurcation analysis of dynamical systems. *Mathematical and Computer Modelling of Dynamical Systems*, 14(2):147175, 2008.
- [10] F. Dumortier and C. Li. Perturbations from an elliptic hamiltonian of degree four. *Journal of Differential Equations*, 175(2):209243, 2001.
- [11] F. Dumortier and C. Li. Perturbation from an elliptic Hamiltonian of degree four-III global centre. *Journal of Differential Equations*, 188(2):473511, 2003.
- [12] F. Dumortier and C. Li. Perturbation from an elliptic Hamiltonian of degree fourIV global centre. *Journal of Differential Equations*, 188(2):512566, 2003.
- [13] F. Dumortier, R. Roussarie, and J. Sotomayor. Generic 3-parameter families of vector fields on the plane, unfolding a singularity with nilpotent linear part. the cusp case of codimension 3. *Ergodic Theory and Dynamical Systems*, 7(03), 1987.
- [14] Freddy Dumortier. *Bifurcations of planar vector fields: nilpotent singularities and Abelian integrals*. Springer-Verlag, Berlin New York, 1991.
- [15] F. Fernández, E. Freire, L. Pizarro, and A.J. Rodríguez-Luis. Proc NDES 96: 4th workshop on nonlinear dynamics of electronic systems (seville, spain). ed J.L. Huertas and A.J. Rodríguez-Luis, page 3216, 1996.
- [16] E. Freire, L. Pizarro, A. J. Rodríguez-Luis, and F. Fernández Sánchez. Multiparametric bifurcations in an enzyme-catalyzed reaction model. *International Journal of Bifurcation and Chaos*, 15(3):905947, 2005.
- [17] E. Freire, L. Pizarro, and A.J. Rodríguez-Luis. Examples of non-degenerate and degenerate cuspidal loops in planar systems. *Dynamics and Stability of Systems*, 14(2):129161, 1999.
- [18] E. Freire, L. Pizarro, and A.J. Rodríguez-Luis. Numerical continuation of homoclinic orbits to non-hyperbolic equilibria in planar systems. *Nonlinear Dynamics*, 23(4):353375, 2000.
- [19] P. Godara, D. Dudkowski, A. Prasad, and T. Kapitaniak. New topological tool for multistable dynamical systems. *Chaos: An Interdisciplinary Journal of Nonlinear Science*, 28(11):111101, nov 2018.
- [20] J. Guckenheimer, R. Rand, and D. Schlomiuk. Degenerate homoclinic cycles in perturbations of quadratic hamiltonian systems. *Nonlinearity*, 2(3):405, 1989.
- [21] Jack Hale. *Dynamics and Bifurcations*. Springer New York, New York, NY, 1991.
- [22] M. Itoh and L.O. Chua. Memristor oscillators. *International Journal of Bifurcation and Chaos*, 18(11):3183–3206, 2008.
- [23] A.I. Khibnik, B. Krauskopf, and C. Rousseau. Global study of a family of cubic lienard equations. *Nonlinearity*, 11(6):1505, 1998.
- [24] L. Kong and C. Zhu. Bogdanov-takens bifurcations of codimensions 2 and 3 in a Leslie-Gower predator-prey model with michaelis-menten-type prey harvesting. *Mathematical Methods in the Applied Sciences*, 40(18):67156731, Mar 2017.
- [25] I.A. Korneev and V.V. Semenov. Andronov- Hopf bifurcation with and without parameter in a cubic memristor oscillator with a line of equilibria. *Chaos: An Interdisciplinary Journal of Nonlinear Science*, 27(8):081104, aug 2017.
- [26] N.V. Kuznetsov, G.A. Leonov, and S.M. Seledzhi. Hidden oscillations in nonlinear control systems. *IFAC Proceedings Volumes*, 44(1):2506–2510, jan 2011.
- [27] G.A. Leonov, N.V. Kuznetsov, and V.I. Vagaitsev. Localization of hidden Chua’s attractors. *Physics Letters A*, 375(23):2230–2233, jun 2011.
- [28] V.K. Melnikov. On the stability of a center for time-periodic perturbations. *Trans. Moscow Math*, 12:1–57, 1963.

- [29] M. Messias, C. Nespoli, and V.A. Botta. Hopf bifurcation from lines of equilibria without parameters in memristor oscillators. *International Journal of Bifurcation and Chaos*, 20(02):437–450, feb 2010.
- [30] E. Ponce, A. Amador, and J. Ros. Unravelling the dynamical richness of 3D canonical memristor oscillators. *Microelectronic Engineering*, 182:15–24, oct 2017.
- [31] A.J. Rodríguez-Luis, E. Freire, and E. Ponce. A method for homoclinic and heteroclinic continuation in two and three dimensions. *Continuation and Bifurcations: Numerical Techniques and Applications*, Springer Netherlands, pages 197–210, 1990.
- [32] S. Schechter. The saddle-node separatrix-loop bifurcation. *SIAM Journal on Mathematical Analysis*, 18(4):11421156, 1987.
- [33] V. Varshney, S. Sabarathinam, A. Prasad, and K. Thamilmaran. Infinite number of hidden attractors in memristor-based autonomous duffing oscillator. *International Journal of Bifurcation and Chaos*, 28(01):1850013, 2018.
- [34] V. Varshney, S. Sabarathinam, K. Thamilmaran, M.D. Shrimali, and A. Prasad. Existence and control of hidden oscillations in a memristive autonomous duffing oscillator. *Nonlinear Dynamical Systems with Self-Excited and Hidden Attractors Studies in Systems, Decision and Control*, page 327344, 2018.
- [35] Stephen Wiggins. *Introduction to applied nonlinear dynamical systems and chaos*. Springer, 2003.
- [36] V. Witte, W. Govaerts, Y. Kuznetsov, and M. Friedman. Interactive initialization and continuation of homoclinic and heteroclinic orbits in MATLAB. *ACM Transactions on Mathematical Software*, 38(3):134, Jan 2012.

Appendix: Dimensional reduction in 3D memristor oscillators

We consider a family of three-dimensional systems, which is general enough to capture all the mathematical models of memristor oscillators given in (30). Such family was been studied in [1] and [30], where the authors showed that the dynamics of such a family of three-dimensional systems is essentially ruled by a one parameter set of two-dimensional systems. We consider the system

$$(46) \quad \begin{aligned} \dot{x} &= a_{11}W(z)x + a_{12}y, \\ \dot{y} &= a_{21}x + a_{22}y, \\ \dot{z} &= x, \end{aligned}$$

where the constants $a_{11}, a_{12}, a_{21}, a_{22} \in \mathbb{R}$ and the function W allows to define a continuous function

$$(47) \quad q(z) = \int_0^z W(s)ds.$$

The next result guarantees that the dynamics of system (46) is essentially two-dimensional, see [1] for a proof.

Proposition 16. *Consider system (46) where the functions W and q are related as in (47). For any $h \in \mathbb{R}$, the set*

$$(48) \quad S_h = \{(x, y, z) \in \mathbb{R}^3 : -a_{22}x + a_{12}y - a_{12}a_{21}z + a_{11}a_{22}q(z) = h\}$$

is an invariant manifold for the system. Therefore, the system has an infinite family of invariant manifolds foliating the whole \mathbb{R}^3 , and so the dynamics is essentially two-dimensional.

In the following result we show that on each invariant set S_h given in (48), and for any continuous function q defined as in (47), the dynamics is topologically equivalent to a Liénard system. Furthermore, we give for any solution of the Liénard system with a given value of h , the corresponding solution of the 3D canonical model (46).

This result is a generalization of Theorem 3 given in [1], where the function q was considered to be a continuous piecewise linear function.

Proposition 17. *Consider system (46) with the function q defined as in (47). If $a_{12} \neq 0$, then on each invariant set S_h given in (48), the dynamics is topologically equivalent to the Liénard system*

$$(49) \quad \dot{X} = Y - F(X), \quad \dot{Y} = -g(X) + h,$$

where F and g are given by

$$(50) \quad F(X) = -a_{11}q(X) - a_{22}X, \quad g(X) = a_{11}a_{22}q(X) - a_{12}a_{21}X$$

Moreover, $(X(\tau), Y(\tau)) \in \mathbb{R}^2$ is a solution of the Liénard system (49) for a given $h \in \mathbb{R}$, if and only if $E_h(X(\tau), Y(\tau)) \in \mathbb{R}^3$ is a solution of system (46) on S_h , where

$$(51) \quad E_h(X(\tau), Y(\tau)) = \begin{pmatrix} Y(\tau) - F(X(\tau)) \\ \frac{1}{a_{12}} [(a_{22}^2 + a_{12}a_{21})Y(\tau) - a_{22}Y(\tau) + h] \\ X(\tau) \end{pmatrix}.$$

Proof. First, with $a_{12} \neq 0$ the change of variables

$$(52) \quad \bar{x} = x, \quad \bar{y} = a_{22}x - a_{12}y, \quad \bar{z} = z$$

transforms system (46) into the system

$$(53) \quad \begin{aligned} \dot{\bar{x}} &= f_1(\bar{z})\bar{x} - \bar{y}, \\ \dot{\bar{y}} &= f_2(\bar{z})\bar{x}, \\ \dot{\bar{z}} &= \bar{x}, \end{aligned}$$

where the functions f_1 and f_2 are defined as

$$(54) \quad f_1(\bar{z}) = a_{11}W(\bar{z}) + a_{22}, \quad f_2(\bar{z}) = a_{22}a_{11}W(\bar{z}) - a_{12}a_{21}.$$

From Proposition 16, the invariant manifolds (48) for system (53)-(54) can be written in the new variables as

$$(55) \quad \tilde{S}_h = \{(\bar{x}, \bar{y}, \bar{z}) \in \mathbb{R}^3 : -\bar{y} + g(\bar{z}) = h\}.$$

Now, replacing the condition given in (55) in the first equation of (53) and removing the unnecessary second equation, we obtain the system

$$(56) \quad \begin{aligned} \dot{\bar{x}} &= f_1(\bar{z})\bar{x} - g(\bar{z}) + h, \\ \dot{\bar{z}} &= \bar{x}. \end{aligned}$$

where the function g is defined by

$$(57) \quad g(u) = a_{11}a_{22}q(u) - a_{12}a_{21}u.$$

After the change of variables

$$(58) \quad \begin{aligned} X &= \bar{z}, \\ Y &= -\tilde{F}(\bar{z}) + \bar{x}, \end{aligned}$$

where F is

$$(59) \quad \tilde{F}(z) = a_{11}q(z) + a_{22}z,$$

we obtain

$$\dot{X} = \dot{\bar{z}} = \bar{x} = Y + \tilde{F}(X) = Y - (-\tilde{F}(X)),$$

so that

$$\begin{aligned}\dot{Y} &= -\tilde{F}'(\bar{z})\dot{\bar{z}} + \dot{\bar{x}} = -(a_{11}q'(\bar{z}) + a_{22}) + (f_1(\bar{z})\bar{x} - g(\bar{z}) + h) = \\ &= -f_1(\bar{z})\bar{x} + f_1(\bar{z})\bar{x} - g(\bar{z}) + h = -g(\bar{z}) + h,\end{aligned}$$

and taking $F(X) = -\tilde{F}(X)$ we obtain system (49)-(50).

If $(X(\tau), Y(\tau)) \in \mathbb{R}^2$ is a solution of system (49)-(50) for a given $h \in \mathbb{R}$, we have from (58) that

$$\begin{pmatrix} \bar{x}(\tau) \\ \bar{z}(\tau) \end{pmatrix} = \begin{pmatrix} Y(\tau) - F(\bar{z}(\tau)) \\ X(\tau) \end{pmatrix}$$

is a solution of system (56). From (55), we obtain on \tilde{S}_h that $\bar{y} = g(\bar{z}) - h$, with g as in (57). Thus,

$$\begin{pmatrix} \bar{x}(\tau) \\ \bar{y}(\tau) \\ \bar{z}(\tau) \end{pmatrix} = \begin{pmatrix} Y(\tau) - F(X(\tau)) \\ g(X(\tau)) - h \\ X(\tau) \end{pmatrix},$$

is a solution of system (53) on S_h . Finally, from (52) we obtain for system (46) the solution $x(\tau) = \bar{x}(\tau)$,

$$\begin{aligned}y(\tau) &= \frac{1}{a_{12}} [a_{22}\bar{x}(\tau) - \bar{y}(\tau)] = \frac{1}{a_{12}} [a_{22}Y(\tau) - a_{22}F(X(\tau)) - g(X(\tau)) + h] \\ &= \frac{1}{a_{12}} [a_{22}Y(\tau) + a_{22}\tilde{F}(X(\tau)) - g(X(\tau)) + h],\end{aligned}$$

and $z(\tau) = \bar{z}(\tau)$. The conclusion follows from the fact that for all X we have

$$a_{22}\tilde{F}(X) - g(X) = (a_{22}^2 + a_{12}a_{21})X.$$

□

In order to apply the analysis performed to system (3), in what follows we consider the function q defined by a cubic polynomial, that is, we assume

$$(60) \quad W(z) = 3cz^2 + 2az + b, \quad q(z) = cz^3 + az^2 + bz,$$

with $c \neq 0$. As a direct consequence of Propositions 16 and 17, we obtain the next result.

Corollary 18. *Consider system (46) with the functions q and W defined as in (60). If $a_{12} \neq 0$, then on each invariant set S_h given by*

$S_h = \{(x, y, z) \in \mathbb{R}^3 : -a_{22}x + a_{12}y + a_{11}a_{22}cz^3 + aa_{11}a_{22}z^2 + (ba_{11}a_{22} - a_{12}a_{21})z = h\}$
the dynamics is topologically equivalent to the Liénard system

$$(61) \quad \begin{aligned}\dot{x} &= y + ca_{11}x^3 + aa_{11}x^2 + (ba_{11} + a_{22})x, \\ \dot{y} &= -a_{11}a_{22}cx^3 - a_{11}a_{22}ax^2 + (a_{12}a_{21} - a_{11}a_{22}b)x + h.\end{aligned}$$

Moreover, $(x(\tau), y(\tau)) \in \mathbb{R}^2$ is a solution of the Liénard system (61) for a given $h \in \mathbb{R}$, if and only if $E_h(x(\tau), y(\tau)) \in \mathbb{R}^3$ is a solution of system (46) on S_h , where

$$(62) \quad E_h(x(\tau), y(\tau)) = \begin{pmatrix} y(\tau) + ca_{11}x(\tau)^3 + aa_{11}x(\tau)^2 + (ba_{11} + a_{22})x(\tau)^2 \\ \frac{1}{a_{12}} [(a_{22}^2 + a_{12}a_{21})y(\tau) - a_{22}y(\tau) + h] \\ x(\tau) \end{pmatrix}.$$

In the next Proposition, we show that system (61) can be written into the form (1).

Proposition 19. *The following statements hold for system (61).*

(a) *If $a_{22} \neq 0$ and $a_{11}a_{22} < 0$ then the system can be written into the form*

$$(63) \quad \dot{x} = y, \quad \dot{y} = \mu_1 + \mu_2 x + cx^3 + \mu_3 y + 3ca_{11}x^2y.$$

where the new parameters μ_1, μ_2 and μ_3 are given by

$$(64) \quad \begin{aligned} \mu_1 &= \frac{27ch + a_{11}a_{22}a(9cb - 2a^2) - 9caa_{12}a_{21}}{27c^2(-a_{11}a_{22})^{5/2}}, \\ \mu_2 &= \frac{a_{11}a_{22}(a^2 - 3cb) + 3ca_{12}a_{21}}{3c(a_{11}a_{22})^2}, \quad \mu_3 = \frac{a_{11}(a^2 - 3cb) - 3ca_{22}}{3ca_{11}a_{22}}. \end{aligned}$$

(b) *If $a_{22} = 0$ then the system can be written into the form*

$$(65) \quad \dot{x} = y, \quad \dot{y} = \mu_1 + \mu_2 x + \mu_3 y + 3ca_{11}x^2y,$$

where the new parameters μ_1, μ_2 and μ_3 are defined by

$$(66) \quad \mu_1 = h - \frac{aa_{12}a_{21}}{3c}, \quad \mu_2 = a_{12}a_{21}, \quad \mu_3 = ba_{11} - \frac{a^2a_{11}}{3c}.$$

Proof. First, the change of variables

$$u = x + \frac{a}{3c}, \quad v = y + \frac{2}{27} \frac{a^3}{c^2} a_{11} - \frac{1}{3} \frac{a}{c} a_{22} - \frac{1}{3} \frac{b}{c} a_{11},$$

transforms system (61) into

$$(67) \quad \begin{aligned} \dot{u} &= v + ca_{11}u^3 + \lambda_1 u, \\ \dot{v} &= -ca_{11}a_{22}u^3 + \lambda_2 u + \lambda_3, \end{aligned}$$

where the new parameters are

$$(68) \quad \begin{aligned} \lambda_1 &= a_{22} + ba_{11} - \frac{1}{3} \frac{a^2}{c} a_{11}, \quad \lambda_2 = a_{12}a_{21} - ba_{11}a_{22} + \frac{1}{3} \frac{a^2}{c} a_{11}a_{22}, \\ \lambda_3 &= h + \frac{1}{3} \frac{b}{c} a_{11}a_{22} - \frac{1}{3} \frac{a}{c} a_{12}a_{21} - \frac{2}{27} \frac{a^3}{c^2} a_{11}a_{22}. \end{aligned}$$

If $a_{11}a_{22} < 0$, the change of variable

$$x = \frac{1}{(-a_{11}a_{22})^{1/2}} u, \quad y = v, \quad \tau = \frac{1}{-a_{11}a_{22}} t,$$

transforms system (67)-(68) into

$$\begin{aligned} \dot{x} &= \frac{1}{(-a_{11}a_{22})^{3/2}} y + ca_{11}x^3 - \frac{\lambda_1}{a_{11}a_{22}} x, \\ \dot{y} &= \frac{\lambda_3}{-a_{11}a_{22}} + \frac{\lambda_2}{(-a_{11}a_{22})^{1/2}} x + c(-a_{11}a_{22})^{3/2} x^3 \end{aligned}$$

and taking into account that

$$\ddot{x} = \frac{1}{(-a_{11}a_{22})^{3/2}} \dot{y} + 3ca_{11}x^2\dot{x} - \frac{\lambda_1}{a_{11}a_{22}} \dot{x},$$

and after some algebra, statement (a) follows.

If $a_{22} = 0$, then from system (67), we obtain statement (b) after a direct computation. \square